EcoHealth 13, 60–71, 2016
DOI: 10.1007/s10393-016-1107-y

ECOHEALTH

Original Contribution

White-Nose Syndrome Disease Severity and a Comparison of Diagnostic Methods

Liam P. McGuire,[1,2] James M. Turner,[1,3] Lisa Warnecke,[1,3] Glenna McGregor,[4] Trent K. Bollinger,[4] Vikram Misra,[5] Jeffrey T. Foster,[6] Winifred F. Frick,[7] A. Marm Kilpatrick,[7] and Craig K. R. Willis[1]

[1]*Department of Biology, University of Winnipeg, 515 Portage Ave., Winnipeg, MB R3B 2E9, Canada*
[2]*Department of Biological Sciences, Texas Tech University, Lubbock, TX 79409*
[3]*Functional Ecology, Biocentre Grindel, University Hamburg, 20146 Hamburg, Germany*
[4]*Canadian Wildlife Health Cooperative, Department of Veterinary Pathology, Saskatoon, SK S7N 5B4, Canada*
[5]*Department of Veterinary Microbiology, University of Saskatchewan, Saskatoon, SK S7N 5B4, Canada*
[6]*Department of Molecular, Cellular, & Biomedical Sciences, University of New Hampshire, Durham, NH 03824*
[7]*Department of Ecology and Evolutionary Biology, University of California Santa Cruz, Santa Cruz, CA 95064*

Abstract: White-nose syndrome is caused by the fungus *Pseudogymnoascus destructans* and has killed millions of hibernating bats in North America but the pathophysiology of the disease remains poorly understood. Our objectives were to (1) assess non-destructive diagnostic methods for *P. destructans* infection compared to histopathology, the current gold-standard, and (2) to evaluate potential metrics of disease severity. We used data from three captive inoculation experiments involving 181 little brown bats (*Myotis lucifugus*) to compare histopathology, quantitative PCR (qPCR), and ultraviolet fluorescence as diagnostic methods of *P. destructans* infection. To assess disease severity, we considered two histology metrics (wing area with fungal hyphae, area of dermal necrosis), *P. destructans* fungal load (qPCR), ultraviolet fluorescence, and blood chemistry (hematocrit, sodium, glucose, pCO_2, and bicarbonate). Quantitative PCR was most effective for early detection of *P. destructans*, while all three methods were comparable in severe infections. Correlations among hyphae and necrosis scores, qPCR, ultraviolet fluorescence, blood chemistry, and hibernation duration indicate a multi-stage pattern of disease. Disruptions of homeostasis occurred rapidly in late hibernation. Our results provide valuable information about the use of non-destructive techniques for monitoring, and provide novel insight into the pathophysiology of white-nose syndrome, with implications for developing and implementing potential mitigation strategies.

Keywords: blood chemistry, histopathology, *Myotis lucifugus*, non-destructive methods, PCR, *Pseudogymnoascus destructans*, ultraviolet fluorescence

Published online: March 8, 2016

Correspondence to: Liam P. McGuire, e-mail: liam.mcguire@ttu.edu

Introduction

White-nose syndrome (WNS) is a fungal disease caused by *Pseudogymnoascus destructans* that affects hibernating bats (Blehert et al. 2009; Lorch et al. 2011; Warnecke et al. 2012; Verant et al. 2014). The fungus grows on exposed skin, penetrates the epidermis, and invades the dermis, resulting in skin lesions (Meteyer et al. 2009). WNS has caused severe declines, including regional extirpation of some species, and has devastated bat populations across eastern and midwestern North America (Frick et al. 2010, 2015; Langwig et al. 2012, 2015b).

The current ''gold-standard'' for diagnosis of WNS is histopathology. Wing tissue is examined for the presence of curved conidia of *P. destructans*, growth of fungal hyphae, and cupping erosions in the epidermis (Meteyer et al. 2009) and a bat may only be confirmed WNS-positive based on these criteria (United States Geological Survey 2014). However, conidia and cupping erosions could be infrequent in mild or early infection, and therefore histological detection of infection may require examination of large amounts of tissue, necessitating euthanasia (but see recent biopsy techniques of Turner et al. 2014). Alternative methods of diagnosing WNS and the presence of *P. destructans* could enable more rapid non-destructive assessment of WNS status and disease severity.

In addition to detecting presence/absence of *P. destructans* and diagnosing disease, quantifying disease severity will be useful for developing and testing hypotheses about pathophysiology. Initial infection with *P. destructans* is not associated with the cupping erosions diagnostic of WNS, and variation in impact among species and populations (Langwig et al. 2012, 2015a, b) suggests that infection may not lead to the development of disease in all individuals or species. However, infection is a precursor of disease in those individuals that later develop cupping erosions so we consider infection an early stage of the disease process. Most WNS studies have documented fungal presence/absence, or compared infected and control groups, but some recent studies have considered disease severity. Reeder et al. (2012) developed a WNS severity score based on histology (presence and extent of *P. destructans* infection and cupping erosions) and found shorter torpor bouts (more frequent arousals) in bats with higher WNS severity scores. Using the same WNS severity score, Cryan et al. (2013) found electrolyte depletion correlated with wing damage, consistent with the hypotonic dehydration hypothesis (Cryan et al. 2010). Warnecke et al. (2013) used a different histology scoring system (proportion of wing with hyphae that had evidence of dermal necrosis) and found lower blood sodium and partial pressure of carbon dioxide (pCO_2) in bats with higher severity scores, contributing to the development of a mechanistic model for the disease. The availability of a variety of disease measures, and an understanding of how they relate to disease severity, will enhance the toolkit available for discerning mechanisms of disease and possible mitigation strategies.

In addition to histology, several non-destructive techniques could be used to assess WNS status and severity, including ultraviolet (UV) fluorescence, quantitative PCR (qPCR), and blood chemistry. Ultraviolet fluorescence has recently been proposed as an indicator of WNS based on orange fluorescence on wing membranes associated with *P. destructans* lesions (Turner et al. 2014). If UV fluorescence correlates with the size and number of lesions, fluorescence could provide a measure of disease severity. Quantitative PCR (Muller et al. 2013) provides an indication of fungal load based on the amount of *P. destructans* DNA detected following standardized swabbing of the forearm, wing, and/or muzzle (Langwig et al. 2015a). Greater fungal loads are likely to increase the probability of lesions and the extent of wing surface area affected by *P. destructans*, which may also indicate disease severity. Finally, blood chemistry could provide an indication of disease severity. Blood sodium (Cryan et al. 2013; Warnecke et al. 2013) and pCO_2 (Warnecke et al. 2013) decrease with increasing WNS severity and several other blood parameters differ between infected (wild or captive inoculated) and uninfected (wild unaffected or captive control) bats, including chloride, hematocrit, glucose, and bicarbonate (Cryan et al. 2013; Warnecke et al. 2013; Verant et al. 2014).

Our objectives were to (1) assess non-destructive diagnostic methods for *P. destructans* infection compared to histopathology, and (2) to evaluate potential metrics of disease severity. We compiled data from three captive inoculation experiments conducted with wild-caught little brown bats (*Myotis lucifugus*). To address the first objective, we compared histological measures, *P. destructans* fungal load, UV fluorescence, and blood chemistry of bats inoculated with *P. destructans* to sham-inoculated control bats. For objective two we examined correlations of various measures, including histology, among inoculated bats. We predicted that fungal load, UV fluorescence, and histology scores would all be greater in inoculated bats compared to controls, and would increase with increasing disease severity. We predicted that bats with higher *P. destructans* fungal

load, UV fluorescence, and histology scores (indicating increased disease severity) would have lower blood sodium, glucose, pCO_2, bicarbonate, and higher hematocrit.

Methods

Data analyzed in this study were gathered from three captive inoculation experiments by the same research team over a 2-year span, and all experiments followed the same general experimental protocol (see summary of experiments in Table 1). Some data from the first experiment have been previously reported (Warnecke et al. 2012, 2013; Wilcox et al. 2014; Turner et al. 2015). All three experiments used hibernating little brown bats collected from WNS-negative hibernacula in central Manitoba, Canada. Bats were placed in cloth bags and transported to the University of Saskatchewan (Saskatoon, SK, Canada) in a temperature-controlled cooler. Upon arrival, the bats were divided into control and treatment groups. Treatment bats were inoculated with 20 μL of a PBS-Tween-20 solution containing ~500,000 *P. destructans* conidia, and control bats were sham-inoculated with 20 μL of PBS-Tween-20 solution lacking conidia as described by Warnecke et al. (2012). Following inoculation, bats were placed into mesh cages in temperature and humidity controlled chambers, provided with ad libitum fresh drinking water, and monitored by infrared motion-sensitive security video. Bats were not disturbed during hibernation other than to remove moribund individuals or for pre-planned removal of bats (see description of third experiment below).

The analysis presented here included a combined total of 181 bats from three experiments. The first experiment (winter 2010–2011; Warnecke et al. 2012) comprised two inoculated (North American and European isolates of *P. destructans*) and one control group ($n = 18$ per group). Environmental chambers were set to 7°C and >97% relative humidity and bats hibernated for 70–118 days. The second experiment (winter 2011–2012) included eight groups—one control and one inoculated group (same North American *P. destructans* isolate as experiment 1) for each of four humidity treatments ($n = 10$ or 11 per group). Environmental chambers were set to 7°C and either 85, 90, 95, or >97% relative humidity and bats hibernated for 48–108 days (all but three bats hibernated >90 days). The third experiment (winter 2011–2012) comprised two groups—one control ($n = 21$) and one inoculated ($n = 23$) with the same North American *P. destructans* isolate as the first experiment. For this experiment, 1/3 of the bats were removed after 36 or 37 days (control and treatment groups, respectively), another 1/3 were removed after 64 or 65 days, and the remaining 1/3 removed at the end of the experiment (days 92 and 93). Overall, methods were very similar in all experiments (same research team, source population, inoculation protocol, environmental chambers, animal cages, and hibernation temperature). The differences among experiments (Table 1) generated a range of disease severity, analogous to the variation likely to be encountered in free-living populations.

In all experiments, bats that showed signs of morbidity (i.e., roosting alone, low in the hibernation cage, with wings partially or completely outstretched; Warnecke et al. 2012) were removed and humanely euthanized. We excluded bats that died prior to being euthanized to avoid complications of changes in diagnostic or physiological variables that might have occurred post-mortem before sample collection. At the end of hibernation (experiment 1 and experiment 2, final sample of experiment 3) or upon scheduled removal (first two samples of experiment 3), bats were euthanized by decapitation under isoflurane anesthesia. Blood was collected with lithium-heparin-treated capillary tubes and whole blood was immediately analyzed with a handheld blood analyzer (i-STAT1 Vet Scan, Abaxis, Union City, California, USA). Blood samples from the first experiment were analyzed with a CG8+ cartridge and samples from the other two experiments were analyzed with an EC8+ cartridge. We considered parameters common to both cartridges and those that differed between inoculated and control bats in the first experiment (Warnecke et al. 2013): sodium, hematocrit, glucose, pCO_2, and bicarbonate (calculated from pH and pCO_2). One blood sodium value from experiment 2 was 3 standard deviations below the mean for that experiment with no other similar data points and, therefore, was excluded as an outlier.

We used standard histological analysis as described by Warnecke et al. (2013). The plagiopatagium of each bat was divided into four sections, 5-μm-thick sections were cut from rolled up wing tissue, stained with periodic acid-Schiff stain, and evaluated with light microscopy. For each bat, we determined the presence or absence of *P. destructans* in the histology samples using published criteria (i.e., curved conidia, hyphal morphology Meteyer et al. 2009; United States Geological Survey 2014).

We used two histology scoring metrics to quantify disease severity. For each wing section, the percentage of skin surface with fungal hyphae was quantified using a six-point scale: 0 (no hyphae), 1 (<1% covered by hyphae), 2 (1–10% hyphae),

Table 1. Summary of the Experiments and Treatment Groups Involved in the Analysis. A total of 181 bats were involved in the three studies. Wing photos of UV fluorescence and qPCR analysis of *P. destructans* fungal load were not collected in experiment 1. Different i-STAT cartridges were used for blood chemistry analysis in experiment 1 than experiments 2 and 3

Experiment	Year	Groups	Inoculation	Sample size	Temperature (°C)	Humidity (RH %)	Duration (days)	Analyses
Experiment 1	Winter 2010–2011	1	NA Pd[a]	18	7	>97	87–113	Histology, i-STAT CG8+
		2	EU Pd[b]	18	7	>97	70–90	Histology, i-STAT CG8+
		3	Control[c]	18	7	>97	118	Histology, i-STAT CG8+
Experiment 2	Winter 2011–2012	1	NA Pd	10	7	85	108	Histology, UV, qPCR, i-STAT EC8+
		2	NA Pd	11	7	90	107	Histology, UV, qPCR, i-STAT EC8+
		3	NA Pd	11	7	95	48–101	Histology, UV, qPCR, i-STAT EC8+
		4	NA Pd	10	7	99	107	Histology, UV, qPCR, i-STAT EC8+
		5	Control	11	7	85	106	Histology, UV, qPCR, i-STAT EC8+
		6	Control	10	7	90	100–105	Histology, UV, qPCR, i-STAT EC8+
		7	Control	10	7	95	105	Histology, UV, qPCR, i-STAT EC8+
		8	Control	10	7	99	106	Histology, UV, qPCR, i-STAT EC8+
Experiment 3	Winter 2011–2012	1a[d]	NA Pd	9	7	99	37	Histology, UV, qPCR, i-STAT EC8+
		1b	NA Pd	7	7	99	65	Histology, UV, qPCR, i-STAT EC8+
		1c	NA Pd	7	7	99	93	Histology, UV, qPCR, i-STAT EC8+
		2a[d]	Control	7	7	99	36	Histology, UV, qPCR, i-STAT EC8+
		2b	Control	7	7	99	64	Histology, UV, qPCR, i-STAT EC8+
		2c	Control	7	7	99	92	Histology, UV, qPCR, i-STAT EC8+

[a] North American isolate of *Pseudogymnoascus destructans*.

[b] European isolate of *Pseudogymnoascus destructans*.

[c] Sham inoculated, lacking fungal conidia.

[d] Experiment 3 involved two cages of bats which were each sampled at 3 time points.

3 (10–30% hyphae), 4 (30–50% hyphae), 5 (>50% hyphae). The same scale was used to quantify the extent of dermal necrosis, considering only areas of the wing with hyphae. We considered extension of disease through the basement membrane and into underlying dermis resulting in necrosis and tissue disruption as a significant stage in pathogenesis. Overall scores for the presence of hyphae were calculated by taking the mid-point of the percentage range corresponding with each score (i.e., 0.5% for a score of 1, 5.5% for a score of 2, etc.) and weighting by the relative size of the corresponding wing section (sections 1 and 2 = 15% of plagiopatagium surface, section 3 = 30%, section 4 = 40%). Overall necrosis scores were calculated similarly, multiplying by the area with hyphae as necrosis was only quantified over the area of the wing with fungal hyphae. Thus, scores for hyphae and necrosis approximate the area of the plagiopatagium affected by each of these metrics.

Our system for scoring disease severity differed somewhat from that published previously because we did not rely on numbers of cupping erosions (Reeder et al. 2012) and, although the overwhelming majority of hyphae was *P. destructans*, our scores were not necessarily *P. destructans*-specific. We used the scoring system described above to account for extensive hyphal growth of *P. destructans* effacing the epidermis without cupping erosions and also to include observations of minor infections with non-*P. destructans* hyphae, both of which could affect pathophysiology. Comparisons of hyphae and necrosis scores between inoculated and control bats also allowed us to quantify non-*P. destructans* hyphae and necrosis, and normal levels of wing injury for healthy hibernating bats.

We obtained ultraviolet wing photos for experiments 2 and 3. After euthanasia, but before necropsy, the dorsal side of the right wing was photographed in a darkened room with a PathStand40 imaging system (SPOT Imaging Solutions, Sterling Heights, MI). The wing was extended across an ultraviolet lightbox (9-W, 368 nm wavelength, model BM100, Way Too Cool LLC, Glendale, AZ) and illuminated from above by two ultraviolet lamps approximately 20 cm above the wing. We quantified percentage of the wing area that fluoresced by outlining the plagiopatagium in ImageJ (version 1.47v) to calculate total surface area, and then manually outlining areas of fluorescence.

Fungal load (*P. destructans*) was determined by qPCR as part of experiments 2 and 3. The forearm and muzzle were swabbed with 5 passes of a sterile polyester swab (Puritan Medical Products; Guilford, ME) moistened with sterile water (Langwig et al. 2015a). The swab was then stored in RNAlater (Sigma-Aldrich; St. Louis, MO) at −20°C. Swabs were packed on dry ice and shipped to the Center for Microbial Genetics & Genomics at Northern Arizona University, where qPCR analysis was performed following Muller et al. (2013). DNA extractions, negative controls, and qPCR followed the methodology detailed in Janicki et al. (2015). Briefly, we used a cycle threshold (C_T) cutoff value of 40 to classify a positive detection of *P. destructans*. Samples were run in duplicate with detection in either duplicate considered positive. We generated a single standard curve on each 96-well qPCR plate with genomic DNA from *P. destructans* ATCC strain MYA-4855, quantified with the Quant-IT PicoGreen double-stranded DNA assay kit (Life Technologies, Carlsbad, CA) in conjunction with a DynaQuant 300 fluorometer (Harvard Bioscience, Inc., Holliston, MA), to confirm that quantifications were consistent from plate to plate. Serial DNA dilutions ranged from 10 ng to 1000 fg. C_T values were converted to nanograms of *P. destructans* DNA based on the following equation $10^{((22.04942-C_T\text{value})/3.34789)}$. One extreme outlier (12 standard deviations greater than the next highest value) was excluded from further analysis.

We compared hyphae and necrosis scores, fluorescence, and *P. destructans* fungal load of inoculated and control bats using non-parametric Mann–Whitney *U* tests because of skewed sample distributions. We compared histological assessment of *P. destructans* presence/absence between inoculated and control bats with a test of proportions. We also calculated the sensitivity (percentage of inoculated bats identified as positive) and specificity (percentage of control bats identified as negative) for presence/absence of *P. destructans*, UV fluorescence, and qPCR to determine their effectiveness as diagnostic criteria. To account for the time course of disease (i.e., bats sampled early in hibernation may not present all symptoms) we also calculated sensitivity and specificity on the subset of bats that had hibernated at least 90 days. We chose this cut-off to include the final sample of experiment 3 but exclude all bats that were sampled early in hibernation as part of experiment 3.

We used t-tests to compare blood parameters of inoculated and non-inoculated bats, including Holm–Bonferroni correction for multiple comparisons. To examine pairwise relationships among diagnostic parameters (fluorescence, qPCR, hyphae, and necrosis scores), we used a Spearman rank correlation matrix because sample distributions were skewed. There were many possible combinations of histology, fluorescence, and qPCR with

blood chemistry variables, so we first examined Pearson correlations to identify relationships for further analysis. Relationships with correlation coefficients >0.2 were examined further using general additive models (GAMs) to quantify non-linear patterns. Smoothing functions in GAMs were fitted using penalized cubic regression splines with the optimal degree of smoothing determined by cross-validation (Zuur et al. 2009). For the relationship between blood sodium and hyphae score, the basis dimension (k) was manually chosen, rather than determined by cross-validation, as the cross-validated solution clearly over-fitted the data. All statistical analysis was performed in the software package R v3.1.0 (R Core Team 2014).

Results

Inoculated bats had greater fluorescence ($W = 412.5$, $P < 0.0001$), *P. destructans* fungal load ($W = 0$, $P < 0.0001$), hyphae score ($W = 1305$, $P < 0.0001$), and necrosis score ($W = 2488.5$, $P = 0.003$) than control bats (Fig. 1). Fungal load, as measured by qPCR, was the most effective diagnostic technique for identifying *P. destructans* infection, correctly identifying all inoculated bats (Fig. 1b; Table 2). Up to 40% of the plagiopatagium area fluoresced on individual inoculated bats (Fig. 1a), but fluorescence was only present on 73% of all inoculated bats and 82% of

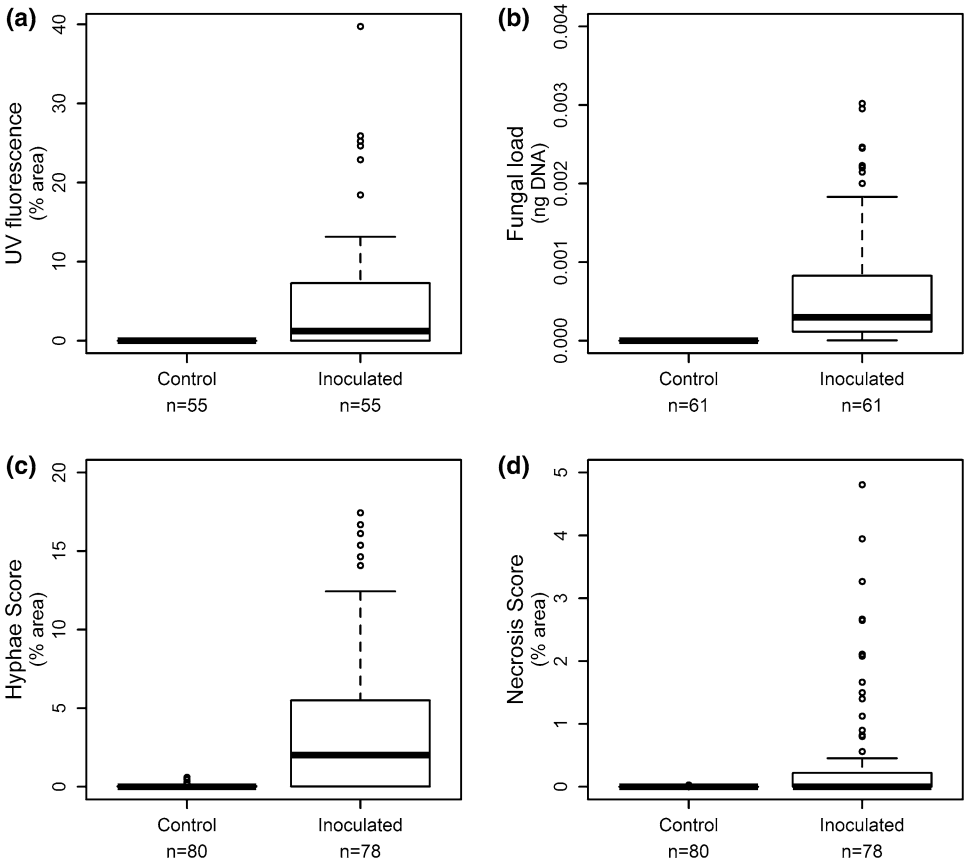

Figure 1. Comparison of inoculated and control bats. Results of statistical comparisons are reported in the text. **a** The percent of the plagiopatagium area that fluoresced. No fluorescence was ever observed on a control bat. **b** *P. destructans* fungal load. No *P. destructans* DNA was ever detected on a control bat. Some control bats showed evidence of fungal hyphae growth (**c**), and necrosis (**d**) but there was no evidence of *Pseudogymnoascus destructans* on any control bats and control histology scores were very low.

Table 2. Comparison of Control and Inoculated Bats for the Diagnostic Factors Considered in the Analysis: UV Fluorescence, *P. destructans* Fungal Load (qPCR), and Histology (Presence/Absence of *P. destructans*). Sensitivity and specificity were calculated with regard to the ability of each method to correctly identify inoculated and control bats. Values in brackets indicate the results when considering the reduced dataset, including only bats that hibernated >90 days

	# Controls	# Inoculated	Sensitivity	Specificity	# False positives	# False negatives
Fluorescence	55 (48)	55 (44)	73% (82%)	100% (100%)	0 (0)	15 (8)
qPCR	61 (47)	61 (43)	100% (100%)	100% (100%)	0 (0)	0 (0)
Histology	80 (66)	78 (53)	73% (85%)	100% (100%)	0 (0)	21 (8)

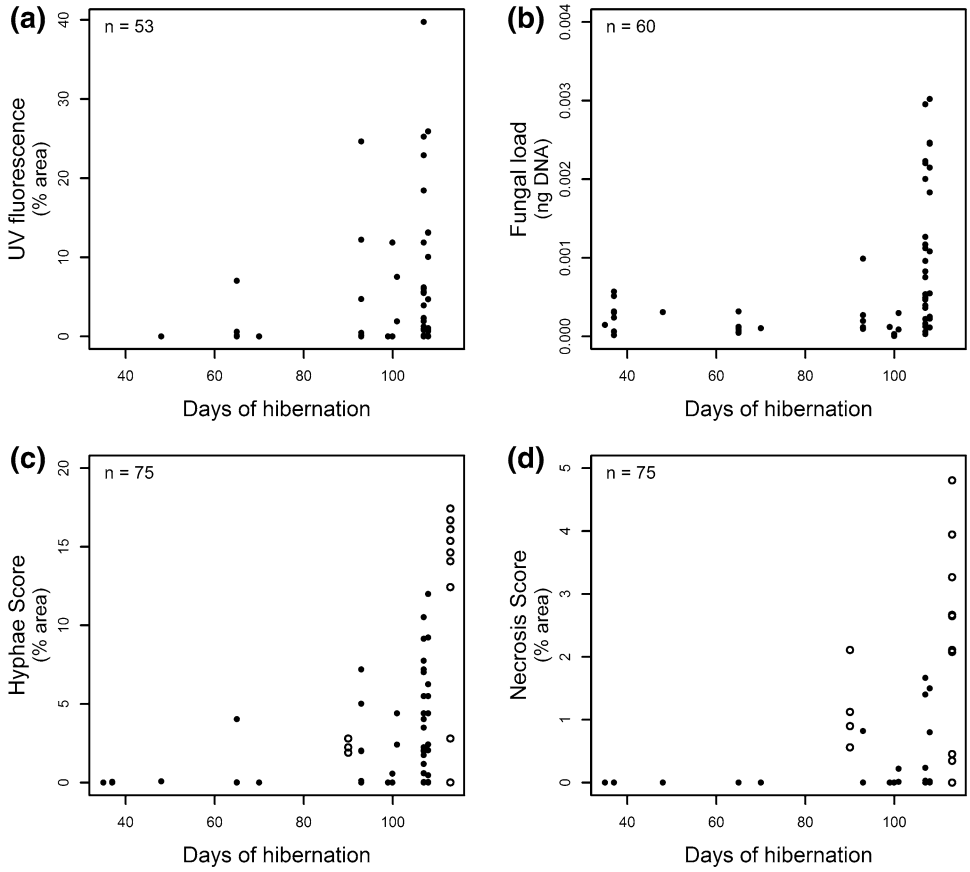

Figure 2. Temporal changes in disease severity metrics of inoculated bats. UV fluorescence (**a**), *P. destructans* fungal load (**b**), hyphae score (**c**), and necrosis score (**d**) increased rapidly late in hibernation. The experiment in year one (*open circles*) continued longer than the experiments in year two (*closed circles*) which likely accounts for the observed year-to-year variation. UV fluorescence and qPCR were not measured in year one.

inoculated bats that hibernated >90 days (Table 2). Histological assessment of the presence or absence of *P. destructans* had identical sensitivity as UV fluorescence (Table 2) with 73% of inoculated bats testing positive for *P. destructans* by histology. As for UV fluorescence, this fraction increased to 85% when only considering bats that hibernated >90 days. All three methods had 100% specificity; no control bats were ever identified as *P. destructans*-positive.

Hyphae and necrosis scores (Fig. 1c, d) were greater in inoculated bats (hyphae: $W = 1305$, $P < 0.0001$; necrosis: $W = 2488.5$, $P = 0.003$). Although non-*P. destructans* hyphae and necrosis were found on some controls (hyphae: 35/80, necrosis: 13/80), these scores were extremely low (hyphae < 0.61, necrosis < 0.04) compared to inoculated bats (mean/max, hyphae: 3.73/17.44, necrosis: 0.43/4.81).

In contrast to earlier analysis using just data from experiment 1 (Warnecke et al. 2013), we found no differences in blood parameters between control and inoculated bats (all $P > 0.10$ after a Holm–Bonferroni correction for multiple comparisons). Disease severity was greater in year one, as indicated by a greater difference between hyphae and necrosis scores of inoculated and control bats in the first year (two-way ANOVA, hyphae: year * inoculation $F_{1,154} = 34.37$, $P < 0.0001$, necrosis: year * inoculation $F_{1,154} = 74.75$, $P < 0.0001$).

In late hibernation, starting at approximately 90 days after inoculation (Fig. 2), there was a dramatic increase in UV fluorescence (rho = 0.37, $S = 15564.55$, $P = 0.006$), *P. destructans* fungal load (rho = 0.51, $S = 17479.37$, $P < 0.0001$), hyphae score (rho = 0.65, $S = 23914.54$, $P < 0.0001$), and necrosis score (rho = 0.43, $S = 40342.75$, $P = 0.0001$).

Spearman rank correlations between all pairwise combinations of UV fluorescence, qPCR, hyphae, and necrosis scores were significant but the strength of these correlations varied (Fig. 3). Relationships between hyphae score and UV fluorescence, hyphae score and *P. destructans* fungal load, and hyphae and necrosis scores were relatively strong (Fig. 3). The relationships between necrosis and UV fluorescence, necrosis and *P. destructans* fungal load, and UV fluorescence and *P. destructans* fungal load were weaker (Fig. 3).

Lower blood sodium concentration was related to higher *P. destructans* fungal loads [Fig. 4a; $P = 0.029$, effective degrees of freedom (edf) = 1.87]. A similar pattern was observed between hyphae score and blood sodium (Fig. 4d; $P < 0.0001$, edf = 2.52) and necrosis score and blood sodium (Fig. 4f; $P < 0.0001$, edf = 6.62). There was

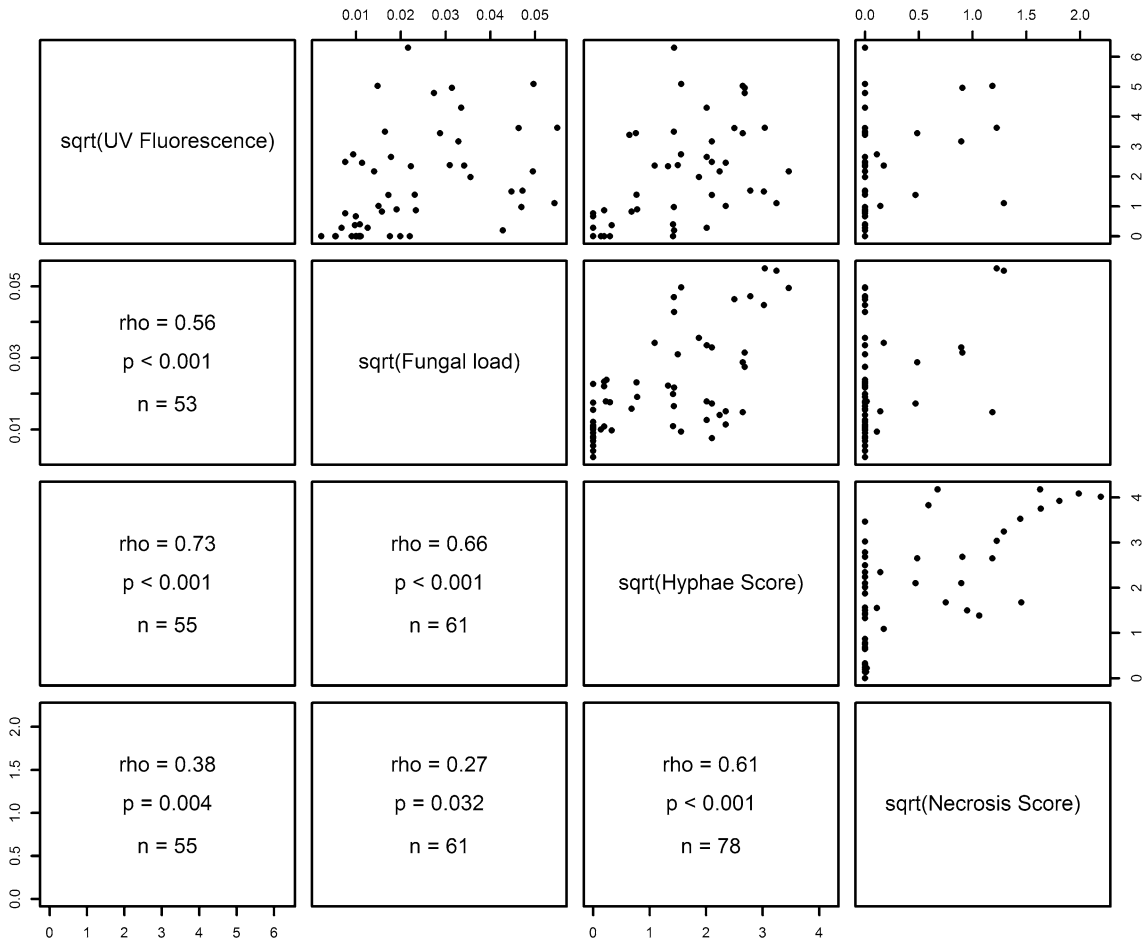

Figure 3. Spearman rank correlation matrix of disease severity metrics. All values have been square root transformed to aid in visual interpretation. Spearman rank correlation rho, *P* value, and sample size are reported below the diagonal, corresponding to the *scatterplots* above the diagonal. Note that UV fluorescence and qPCR were not measured in experiment 1.

a weak trend for a reduction in pCO_2 at higher *P. destructans* fungal loads but the relationship was not significant (Fig. 4b; $P = 0.125$). However, pCO_2 did decrease with hyphae score (Fig. 4e; $P = 0.0012$, edf = 2.25) and necrosis score (Fig. 4g; $P = 0.0005$, edf = 2.67). The opposite pattern was apparent for the relationship between *P. destructans* fungal load and bicarbonate. At higher *P. destructans* fungal loads, bicarbonate concentration increased (Fig. 4c; $P = 0.0079$, edf = 2.22). UV fluorescence was not correlated with any blood parameters.

Discussion

Compared to UV fluorescence and histology, qPCR was most effective at determining *P. destructans* infection status (100% sensitivity, 100% specificity), even in early hibernation when fungal load and disease severity were low. Histology and UV fluorescence were similar in differentiating inoculated bats from controls, and were similar to qPCR for bats with advanced infection that had hibernated >90 days. Importantly, none of the methods (qPCR, UV fluorescence, or histology) resulted in false positives (i.e., control bats identified as positive). Therefore, except during early winter or cases where fungal infection does not lead to the development of lesions, UV provides a useful field method for identifying infected bats (Turner et al. 2014) that is complementary to visual surveys (Janicki et al. 2015). Both qPCR and UV represent effective ways to rapidly and non-destructively sample bats for presence of *P. destructans*, although qPCR performs best at all stages of infection. UV fluorescence and fungal load were correlated with hyphae score (Fig. 3) and thus may be useful as metrics of disease severity. While UV fluorescence was poorly correlated with necrosis score, this could reflect the fact that, in contrast to other metrics, we were not able to

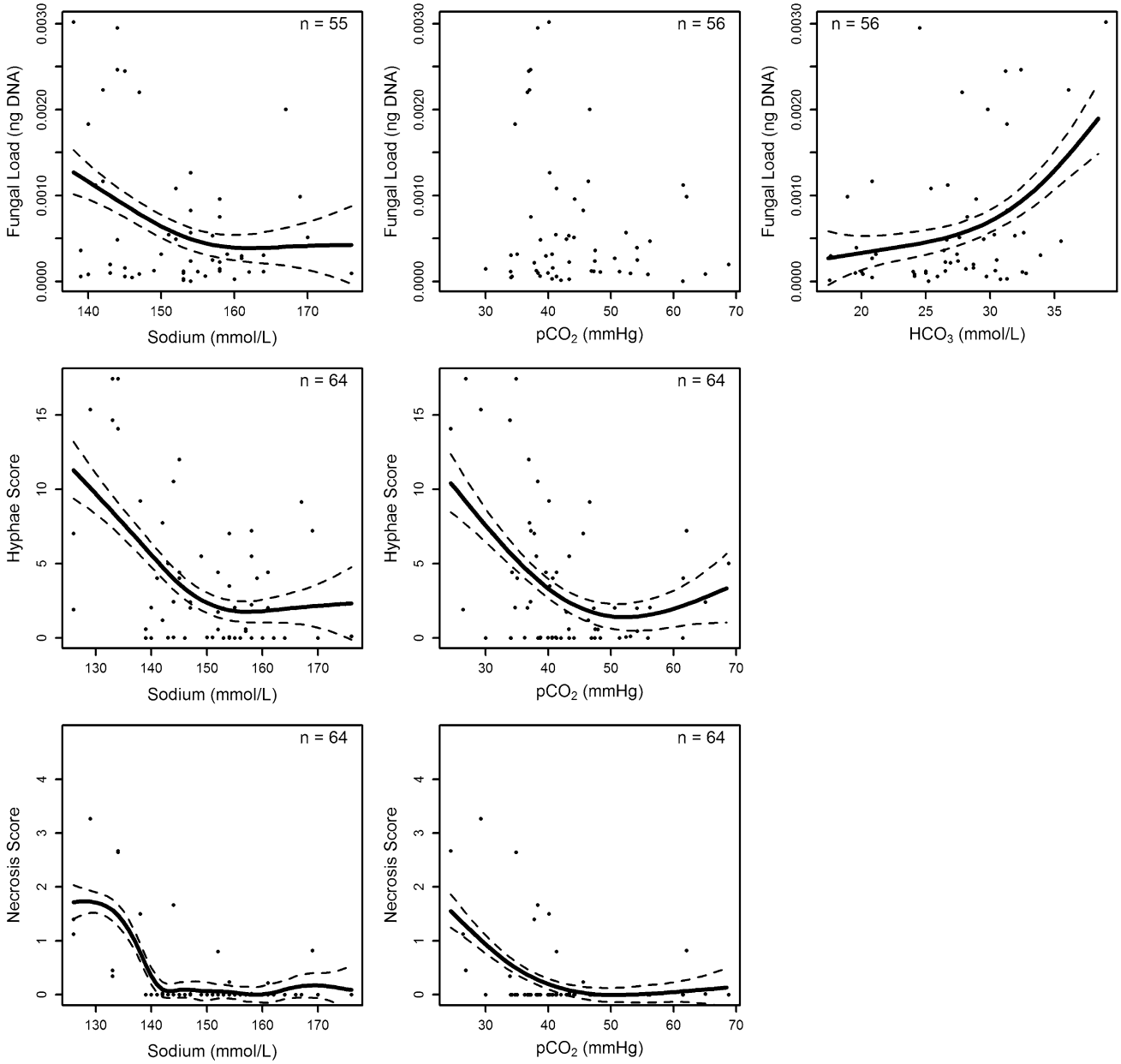

Figure 4. General additive models fitted to non-linear relationships among blood and disease severity metrics. *Solid line* indicates the model fit and *dashed lines* indicate ±1 standard error. The relationship between pCO_2 and *P. destructans* fungal load met the criteria for examination with GAM (see text), but there was no significant relationship.

collect data on UV fluorescence for bats in our dataset with the most severe disease (i.e., year 1). Thus, we recommend additional studies of UV fluorescence in bats with advanced infections.

Histology scores for control bats with non-zero hyphae and necrosis scores were extremely low (Fig. 1) and large quantities of hyphal growth and necrosis were only observed in bats inoculated with *P. destructans*. False negatives (i.e., inoculated bats with zero scores for hyphae and necrosis) likely reflect early stages of disease progression in which hyphae have not yet proliferated across sufficient areas of the wing to be detected. Most false negatives (16/22) were from experiment 3 during which bats were removed in early-mid hibernation. Increasing the number of histological sections examined would increase sensitivity and potentially help identify individuals in the early stages of disease that have not yet developed widespread lesions, but would be costly and time consuming.

The non-linear patterns we observed between blood chemistry and other measures of fungal growth or pathol-

ogy (Fig. 4) suggest a multi-stage progression of disease. During early stages of infection physiological consequences are not severe, but as hyphae proliferate in the epidermis they involve sufficient area of the wing surface to impair function. As infection progresses, fungal hyphae also begin to penetrate the basement membrane of the epidermis causing dermal necrosis. In later stages of infection, blood sodium and pCO_2 are reduced, and bicarbonate becomes elevated. The positive relationship between *P. destructans* fungal load and bicarbonate apparently contradicts the treatment effect (lower bicarbonate in inoculated bats) reported by Warnecke et al. (2013). *P. destructans* fungal load was only available in year 2 when there was no inoculation effect on bicarbonate. Numerous factors may affect bicarbonate concentration and these observations require further investigation. Hibernation duration may account for the difference we observed between years for histology and blood analyses. The majority of the bats in year 1 (88%, 28/32) survived for >108 days of hibernation, which was the maximum hibernation duration in year 2. Thus, our dataset was dominated by bats in early stages of infection with lower disease severity. With a larger sample of severely diseased animals (perhaps following longer hibernation duration) stronger relationships between variables such as fluorescence and necrosis score may become apparent.

The rapid increase in many of the variables we measured late in hibernation (Fig. 2), and the patterns we observed for disease severity (Fig. 2), could be informative for management. Our data suggest that rather than a gradual increase in the severity of symptoms throughout hibernation, WNS is characterized by a dramatic disruption of homeostasis that happens quickly, late in hibernation. These observations are consistent with Verant et al. (2014) where the hibernation period was shorter (98 days compared with up to 118 days) and severe disease was not observed. In situations where the hibernation period is shorter (e.g., southern latitudes) or where microclimate or social conditions limit fungal growth or transmission (Langwig et al. 2012; Verant et al. 2012), there may be an increased likelihood of survival and recovery from the disease. In regions where hibernation durations are long and/or the fungus grows quickly, bats may be more likely to reach the advanced phase of disease, with numerous homeostatic factors disrupted, and increased likelihood of mortality or reduced likelihood of recovery in bats that survive to spring emergence. This temporal pattern of disease progression could be important when considering mitigation strategies. For example, management options requiring the application of some treatment (Cornelison et al. 2014; Hoyt et al. 2015) should consider how disease progression might affect the optimal timing of treatment application.

Several studies have documented the lesions and increased arousals caused by *P. destructans* infection, and have suggested that increased arousals lead to premature depletion of energy stores (Cryan et al. 2010; Warnecke et al. 2012; Reeder et al. 2012; Warnecke et al. 2013; Verant et al. 2014). What is still not understood are the pathophysiological connections between lesions in wing tissue and increased arousal frequency, and other disease processes that may contribute to mortality. Consideration of disease severity and the chronology of disease-related pathologies are critical next steps for developing an integrated understanding of WNS, with potential disease management applications in both free-living (e.g., comparisons among affected sites) and captive contexts (e.g., targeting individuals for rehabilitation). The pattern of disease severity we observed and abrupt changes in diagnostic measures during late hibernation suggest that simply comparing inoculated (i.e., sick) versus control (i.e., healthy) bats may be misleading without accounting for some index of disease severity.

Conclusion

Our results highlight the value of non-destructive sampling methods, and the potential for these methods to diagnose *P. destructans* infection and quantify disease severity, in the context of monitoring disease progression. Minimally invasive, non-lethal sampling techniques can allow for powerful longitudinal studies, tracking disease progression within individuals and monitoring disease processes in free-living animals. Until we understand fully the processes by which infection with *P. destructans* harms the host, mitigation options will be limited. However, techniques such as those described here provide important tools to develop a more complete understanding of variation in disease severity and the chronology of disease progression.

Acknowledgments

We thank the animal care staff (Monique Burmester, Paula Mason, Melanie Weiss), imaging specialists (Ian Shirley, Chris Stuart), and necropsy team (Marnie Zimmer, Crystal Rainbow) at the Western College of Veterinary Medicine for their support and technical expertise throughout these

studies. We also thank Katy Parise, Nicolette Janke, and Kevin Drees at the Center for Microbial Genetics and Genomics at Northern Arizona State University for molecular diagnostics. Funding was provided by the United States Fish and Wildlife Service, Canada Foundation for Innovation, Manitoba Research and Innovation Fund, Natural Sciences and Engineering Research Council of Canada, the German Academic Exchange Service (DAAD), and NSF grant DEB-1115895.

Ethical Approval

All applicable institutional and/or national guidelines for the care and use of animals were followed. Collection of wild bats was approved under permits from Manitoba Conservation (Permits WB11145 and WB13148) and experiments were approved by the University of Saskatchewan Committee on Animal Care and Supply (Protocol #20100120).

References

Blehert DS, Hicks AC, Behr M, Meteyer CU, Berlowski-Zier BM, Buckles EL, Coleman JTH, Darling SR, Gargas A, Niver R, Okoniewski JC, Rudd RJ, Stone WB (2009) Bat white-nose syndrome: an emerging fungal pathogen. *Science* 323:227

Cornelison CT, Keel MK, Gabrial KT, Barlament CK, Tucker TA, Pierce GE, Crow SA Jr (2014) A preliminary report on the contact-independent antagonism of *Pseudogymnoascus destructans* by *Rhodococcus rhodochrous* strain DAP96253. *BMC Microbiology* 14:246

Cryan PM, Meteyer CY, Boyles JG, Blehert DS (2010) Wing pathology of white-nose syndrome in bats suggests life-threatening disruption of physiology. *BMC Biology* 8:135

Cryan PM, Meteyer CU, Blehert DS, Lorch JM, Reeder DM, Turner GG, Webb J, Behr M, Verant M, Russell RE, Castle KT (2013) Electrolyte depletion in white-nose syndrome bats. *Journal of Wildlife Diseases* 49:398–402

Frick WF, Pollock JF, Hicks AC, Langwig KE, Reynolds DS, Turner GG, Butchkoski CM, Kunz TH (2010) An emerging disease causes regional population collapse of a common North American bat species. *Science* 329:679–682

Frick WF, Puechmaille SJ, Hoyt JR, Nickel BA, Langwig KE, Foster JT, Barlow KE, Bartonicka T, Feller D, Haarsma AJ, Herzog C, Horacek I, van der Kooij J, Mulkens B, Petrov B, Reynolds R, Rodrigues L, Stihler CW, Turner GG, Kilpatrick AM (2015) Disease alters macroecological patterns of North American bats. *Global Ecology and Biogeography* 24:741–749

Hoyt JR, Cheng TL, Langwig KE, Hee MM, Frick WF, Kilpatrick AM (2015) Bacteria isolated from bats inhibit the growth of *Pseudogymnoascus destructans*, the causative agent of white-nose syndrome. *PLoS One* 10:e0121329

Janicki AF, Frick WF, Kilpatrick AM, Parise KL, Foster JT, McCracken GF (2015) Efficacy of visual surveys for white-nose syndrome at bat hibernacula. *PLoS One* 10:e0133390

Langwig KE, Frick WF, Bried JT, Hicks AC, Kunz TH, Kilpatrick AM (2012) Sociality, density-dependence and microclimates determine the persistence of populations suffering from a novel fungal disease, white-nose syndrome. *Ecology Letters* 15:1050–1057

Langwig KW, Frick WF, Reynolds R, Parise KL, Drees KP, Hoyt JR, Cheng TL, Kunz TH, Foster JT, Kilpatrick AM (2015) Host and pathogen ecology drive the seasonal dynamics of a fungal disease, white-nose syndrome. *Proceedings of the Royal Society B: Biological Sciences* 282:20142335

Langwig KE, Hoyt JR, Parise KL, Kath J, Kirk D, Frick WF, Foster JT, Kilpatrick AM (2015) Disease dynamics of white-nose syndrome invasion, Midwest USA. *Emerging Infectious Diseases* 21:1023–1026

Lorch JM, Meteyer CU, Behr MJ, Boyles JG, Cryan PM, Hicks AC, Ballmann AE, Coleman JTH, Redell DN, Reeder DM, Blehert DS (2011) Experimental infection of bats with *Geomyces destructans* causes white-nose syndrome. *Nature* 480:376–379

Meteyer CU, Buckles EL, Blehert DS, Hicks AC, Green DE, Shearn-Bochsler V, Thomas NJ, Gargas A, Behr MJ (2009) Histopathologic criteria to confirm white-nose syndrome in bats. *Journal of Veterinary Diagnostic Investigation* 21:411–414

Muller LK, Lorch JM, Lindner DL, O'Connor M, Gargas A Blehert DS (2013) Bat white-nose syndrome: a real-time TaqMan polymerase chain reaction test targeting the intergenic spacer region of *Geomyces destructans*. *Mycologia* 105:253–259

R Core Team (2014) R: a language and environment for statistical computing. R Foundation for Statistical Computing, Vienna, Austria. http://www.R-project.org/.

Reeder DM, Frank CL, Turner GG, Meteyer CU, Kurta A, Britzke ER, Vodzak ME, Darling SR, Stihler CW, Hicks AC, Jacob R, Grieneisen LE, Brownlee SA, Muller LK, Blehert DS (2012) Frequent arousal from hibernation linked to severity of infection and mortality in bats with white-nose syndrome. *PLoS One* 7:e38920

Turner JM, Warnecke L, Wilcox A, Baloun D, Bollinger TK, Misra V, Willis CKR (2015) Conspecific disturbance contributes to altered hibernation patterns in bats with white-nose syndrome. *Physiology and Behavior* 140:71–78

Turner GG, Meteyer CU, Barton H, Gumbs JF, Reeder DM, Overton B, Bandouchova H, Bartonička T, Martínková N, Pikula J, Blehert DS (2014) Nonlethal screening of bat-wing skin with the use of ultraviolet fluorescence to detect lesions indicative of white-nose syndrome. *Journal of Wildlife Diseases* 50:566–573

United States Geological Survey, National Wildlife Health Center (2014) Updated WNS case definitions. https://www.whitenosesyndrome.org/resource/revised-case-definitions-white-nose-syndrome-11252014. Accessed 29 July 2015.

Verant ML, Boyles JG, Waldrep W Jr, Wibbelt G, Blehert DS (2012) Temperature-dependent growth of *Geomyces destructans*, the fungus that causes bat white-nose syndrome. *PLoS One* 7:e46280

Verant ML, Meteyer CU, Speakman JR, Cryan PM, Lorch JM, Blehert DS (2014) White-nose syndrome initiates a cascade of physiologic disturbances in the hibernating bat host. *BMC Physiology* 14:10

Warnecke L, Turner JM, Bollinger TK, Lorch JM, Misra V, Cryan PM, Wibbelt G, Blehert DS, Willis CKR (2012) Inoculation of bats with European *Geomyces destructans* supports the novel pathogen hypothesis for the origin of white-nose syndrome. *Proceedings of the National Academy of Sciences* 109:6999–7003

Warnecke L, Turner JM, Bollinger TK, Misra V, Cryan PM, Blehert DS, Wibbelt G, Willis CKR (2013) Pathophysiology of white-nose syndrome in bats: a mechanistic model linking wing damage to mortality. *Biology Letters* 9:20130177

Wilcox A, Warnecke L, Turner JM, McGuire LP, Jameson JW, Misra V, Bollinger TC, Willis CKR (2014) Behaviour of hibernating little brown bats experimentally inoculated with teh pathogen that causes white-nose syndrome. *Animal Behaviour* 88:157–164

Zuur AF, Ieno EN, Walker NJ, Saveliev AA, Smith GM (2009) *Mixed effects models and extensions in ecology with R*, New York: Springer